An Efficient Method for Aiming Heliostats Using Ray-tracing

Shuang Wang[1], Charles-Alexis Asselineau[1], John Pye[1] and Joe Coventry[1,*]

Research School of Electrical, Energy and Materials Engineering, Australian National University, Canberra

In a solar power tower plant, the role of the heliostat aiming strategy is to control the radiative flux distribution at the receiver surface to avoid thermally induced damage, while minimising spillage losses and maximising the receiver thermal efficiency [1,2]. Flux limitations arise from factors including the heat transfer fluid stability limits, and thermo-mechanical stress limits in receiver pipes. Thermal efficiency is maximised when the flux is high, and as close as possible to local flux limits. The Image Size Priority method was developed to sequentially optimise aiming points of single heliostats, using fast convolution-based optical simulations to evaluate individual flux maps [3]. However, to accurately determine receiver flux distributions, ray tracing is preferred. Ray tracing is computationally expensive and determination of the aim points for every heliostat independently potentially leads to impractical simulation times. In this study, we introduce a new parameterisation of heliostat aim-point locations that significantly reduces the number of parameters to determine. Based on the deviation-based aiming strategy suggested by Augsburger [4], it enables efficient use of ray-tracing to optimise the aiming strategy and, together with receiver thermal and mechanical models, is able to closely match the flux distribution to local values of allowable flux on the receiver. A reference case with a surrounding field and a cylindrical external receiver compatible with the Gen3 Liquid Pathway project is presented to test the capability of the method developed in this study.

1. The modified deviation-based methods

The principle of the deviation-based method is that heliostats with the tightest focal spot aim at the boundaries of the receiver, while those with the largest focal spot aim at the centre line. The original method excludes a vertically asymmetric flux. A modified deviation-based aiming (MDBA) method is proposed in this study to improve the capabilities of the existing method. All heliostats are divided into sectors according to their azimuth angles, with each sector aiming at one tube bank, as shown in Figure 1. Heliostats within each sector are ranked in ascending focal distance order, and the aiming point for heliostat *i* in sector *j* is determined:

$$z^{\#,\&}_{\text{"\#\$}} = z_{\text{"\#\$}} + M_{\#,\&}\,0.5E_{\&}H_{/01}\,2\,\frac{f_{\$\text{"}4,\&} - f_{\#,\&}}{f_{\$\text{"}4,\&} - f_{\$\#6,\&}}\,7^{8_9}, i = 1,\dots,N_{>?@,\&}, j = 1,\dots,N_{\text{B"6C}} \quad (1)$$

$$x_{\text{"\#\$}} = \frac{x_{>?@} \times R_{/01}}{\sqrt{x_{>?@}^{J} + y_{>?@}^{J}}},\ y_{\text{"\#\$}} = \frac{y_{>?@} \times R_{/01}}{\sqrt{x_{>?@}^{J} + y_{>?@}^{J}}} \quad (2)$$

where E_j is the aiming extent for sector *j*, which determines the fraction of the receiver that can be targeted with aim points. $f_{max,j}$ and $f_{min,j}$ are the maximum and minimum focal distances of all heliostats in sector *j*. S_j is defined as the shape exponent and controls the shape of the vertical flux distribution. $M_{i,j}$ is the index matrix. The index matrix assigns individual heliostat aim points to the upper or lower part of the receiver. The matrix indices are controlled by an asymmetry factor A_j, which defines the ratio of heliostats targeting at the upper section of the receiver ($N_{hst,up}$) to total heliostats (N_{hst}): $A_j = N_{hst,up} / N_{hst}$. In total, the aiming points for all heliostats in sector *j* are determined by the aiming extent (E_j), the shape exponent (S_j), and the asymmetry factor (A_j). For the reference case with 16 field sectors, the number of parameters is 16×3=48.

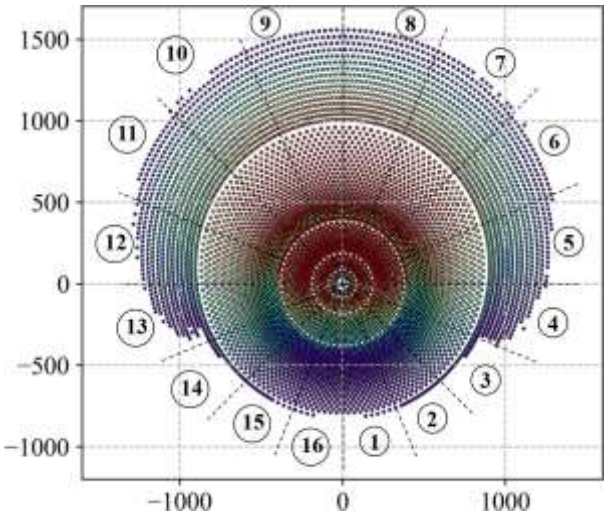

Figure 1 Division of the heliostat field into sectors

2. Models and methodology

The referenced receiver is composed of 16 tube banks and eight flow paths with north top injection and south top exit. The total radius and height of the receiver are 16 m and 24 m, respectively. The tube material is alloy 740H. The field layout locates in Dagget, CA, and is composed of 6764 heliostats. A thermal output of 543 MW can be generated at design point (equinox solar noon). The optical simulation is executed using ray-tracing as implemented in the SOLSTICE open-source software [5]. The receiver thermal model used is from Asselineau [6] and the temperature and mass flow dependent flux limits are evaluated using the model proposed by Logie et al. [7].

3. Comparison of MDBA optimisation methods

Different methods have been explored to solve the optimisation problem. The first approach is an optimisation-based method. In this approach, the objective is to minimise the negative value of the interception efficiency ($-\eta_{int}$), with a constraint condition such that no crossover occurs. The optimisation method is chosen as a pattern search method, and the ending criterion is that the pattern size is contracted to 0.1 of the primary size. The optimisation has been implemented with no division and by dividing the problem into 4, 8 and 16 sub-problems, each sub-problem considering 4, 2 and 1 sector(s), respectively. The results are shown in Table 1. All the four cases can obtain the aiming points controlling the net flux under the limit. Figure 2 illustrates an example of the flux curves for case O1. The trends of the net flux curves match well with the limit curves. The interception efficiencies drop by 0.5% to 0.8% compared to the equatorial aiming (η_{int}=97.0%). However, this approach is too time-consuming with more than 785 instances of evaluation of ray-tracing. Figure 3 shows the process of the optimisation in case O1. The objective function gradually drops with the number of evaluation until the ending criterion is met.

Table 1 Results of the optimisation-based method

Case	Number of parameters	Number of sub-problems	Optimum efficiency	Number of evaluation	Number per sub-problem	Description
O1	48	1	96.5%	3082	3082	For all sectors
O2	12	4	96.4%	1413	353	For two flow paths
O3	6	8	96.4%	1184	148	For single flow path
O4	3	16	96.2%	785	49	For single tube bank

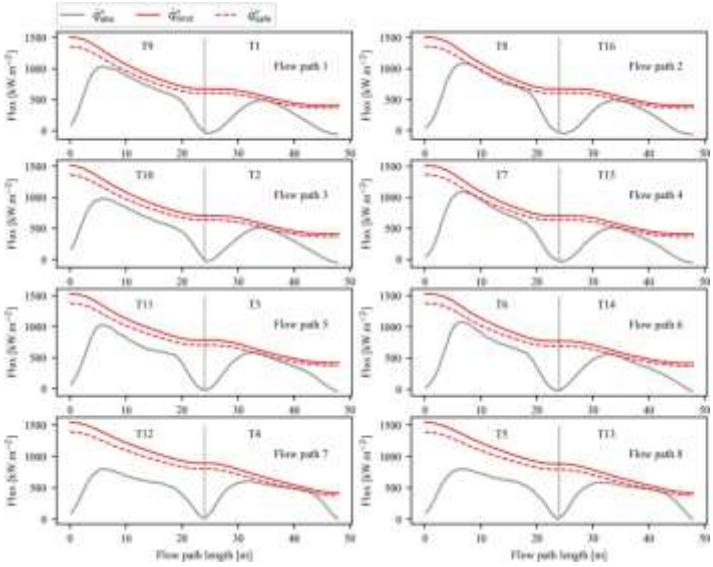

Figure 2 Curves of net flux and flux limit for different flow paths (case O1)

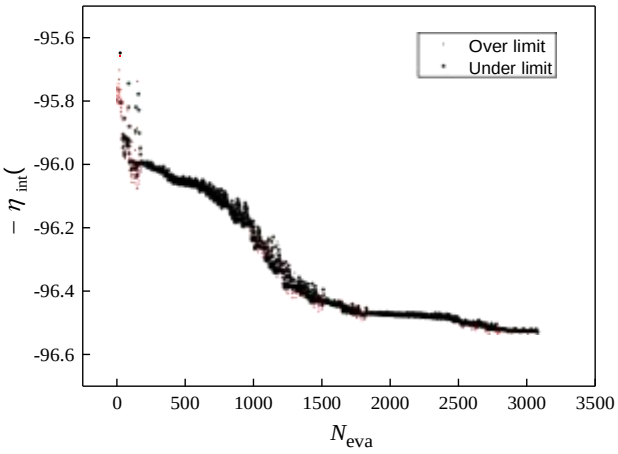

Figure 3 Process of the optimisation (case O1)

The second approach is a sequential method. Preliminary aiming extents are searched in the first step with a vertically symmetric flux profile [8], and the second step is to reduce the cross-over extents to zero by optimising shape exponents and asymmetry factors. The constraint condition is that the interception efficiency does not drop by 1.0% in relative terms compared to equatorial aiming. Table 2 shows the results for the sequential method with different divisions. The curves of net flux and flux limits for case S4 are illustrated in Figure 4.

Table 2 Results of the sequential method

Case	Number of parameters	Number of sub-problems	Optimum efficiency	Number of evaluation	Number per sub-problem	Description
S1	32	1	96.5%	192	32	For all sectors
S2	8	4	96.5%	37	8	For two flow paths
S3	4	8	96.4%	34	4	For single flow path
S4	2	16	96.5%	32	2	For single tube bank

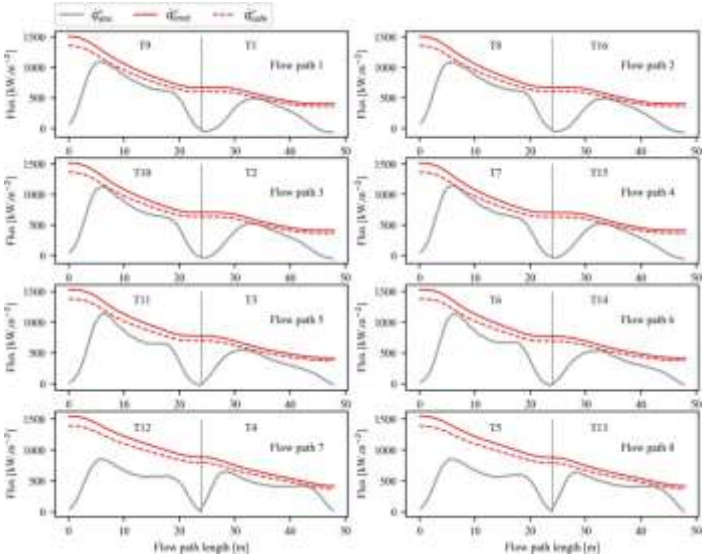

Figure 4 Curves of net flux and flux limit for different flow paths (case S4)

As shown in the results, the optimum interception efficiencies are almost equivalent to case O1, while the numbers of instances of ray-tracing evaluation are significantly reduced. The benefit of the interception efficiency mainly comes from the preliminary search of aiming extents, which results in a good initial point for the optimisation in the second step. The optimisation problems quickly end once the cross-over extents are reduced to zero and do not fall into the slow minimisation process as in Figure 3. For case S4, the simulation takes about ten minutes with ray number of 10^7 on a desktop PC with i7 processors and 16 GB ram.

References

[1] Besarati, S.M., Goswami, D.Y., Stefanakos, E.K., 2014, 'optimal heliostat aiming strategy for uniform distribution of heat flux on the receiver of a solar power tower plant', Energy Convers Manag, 84, pp.234–43.

[2] Ashley, T., Carrizosa, E., Fernández-Cara, E., 2017, 'optimisation of aiming strategies in solar power tower plants', Energy, 137, pp.285-291.

[3] Wagner, M.J., Wendelin, T., 2018, 'SolarPILOT: A power tower solar field layout and characterization tool', Sol Energy, 171, pp.185–196.

[4] Augsburger, G., Thermo-economic optimisation of large solar tower power plants, 2013.

[5] Caliot, C., Benoit, H., Guillot, E., et al., 2015, 'Validation of a Monte Carlo integral formulation applied to solar facility simulations and use of sensitivities', J. Sol. Energy Eng. Trans. ASME, 137(2).

[6] Asselineau, C.A., Geometrical optimisation of receivers for concentrating solar thermal systems, 2017.

[7] Logie, W.R., Pye, J.D., Coventry, J., 2018, 'Thermoelastic stress in concentrating solar receiver tubes: A retrospect on stress analysis methodology, and comparison of salt and sodium', Sol Energy, 160, pp.368-379.

[8] Sánchez-González, A., Rodríguez-Sánchez, M.R., Santana, D., 2017, 'Aiming strategy model based on allowable flux densities for molten salt central receivers', Sol Energy, 157, pp.1130-1144.